Accepted manuscript, DOI of final publication: 10.1016/j.precisioneng.2012.06.001

DIAMOND MICRO CHISELING OF LARGE-SCALE RETROREFLECTIVE ARRAYS

Ekkard BRINKSMEIER, Ralf GLÄBE and Lars SCHÖNEMANN

LFM - Laboratory for Precision Machining, Badgasteiner Straße 2, 28359 Bremen, Germany

Corresponding Author:

Lars Schönemann
LFM - Laboratory for Precision Machining
Badgasteiner Straße 2
28359 Bremen, Germany
schoenemann@lfm.uni-bremen.de
phone +49 421 218 51142
fax +49 421 218 51119

Abstract:

Triple mirror retroreflectors are essential components for safety applications, communications and measurement equipment. While downscaling of characteristic dimension is possible for triangular retroreflectors, this is a challenging task for full-cube retroreflectors, due to the absence of continuous tool paths. Thus, the Diamond Micro Chiseling (DMC) process has been developed which allows the machining of full-cube retroreflectors by overlapping a series of sharp-edged pyramidal microcavities. In the past, this has been successfully demonstrated on a small-scale up to 3 x 3 mm² with a structure size of 150 µm. Industrial applications, however, require the structuring of areas which are significantly larger than 10 x 10 mm².

This paper will introduce the technology for machining such pattern with the help of the DMC process. Particular attention will be given to the measurement procedures and required tolerances for performing an in-situ tool change as well as the optimization strategies for reducing the required process time.

Keywords: Precision Machining, Retroreflective Surface, Functional Surfaces, Diamond Micro Chiseling

Accepted manuscript, DOI of final publication: 10.1016/j.precisioneng.2012.06.001

1 Introduction

The manufacture of microstructures has been in focus of many recent research projects, as they can be used to enhance technical surfaces with all kinds of additional functionalities [1-3] and thus are driving advances in many fields of application [4-6].

A special type of optical structures are retroreflective surfaces which act as functional features for safety applications [7], communications [8] and measurement [9] equipment. They can be manufactured as a combination of lens and mirror (cat's-eye retroreflector) or in the form of triple mirrors with perpendicular facets (cube corners) [10]. Lens and mirror reflectors are mainly used in security applications because they offer a greater acceptance angle of the incident light. Triple mirror structures are preferred in measurement applications, as a smaller amount of the incident light is lost due to scattering effects [11]. In most applications, multiple of these structures are combined in an array to form a retroreflecting surface. According to the geometry of the mirror facets, it is distinguished between retroreflectors with triangular (i.e. triangular facets) or hexagonal (i.e. cubic facets) aperture. Other types of triple mirror retroreflectors (e.g. polyhedrons [12]) are also sometimes used to improve the retroreflective performance, but are comparatively uncommon. In this paper, the term hexagonal or triangular retroreflector describes an array of the abovementioned triple mirror structures.

Smaller structures result in a lower parallel displacement of the reflected light and thereby allow smaller measurement devices and improved performance. Reducing the structure size of hexagonal retroreflectors is of particular interest, as they provide 100 % efficiency at 0° incidence compared to approximately 66 % with triangular retroreflectors (see Figure 1) [13]. Furthermore, when replicating an array of miniaturized structures on reflective foils, the retroreflective surface can be bent without loss of optical function and thus offer a broader range of applications.

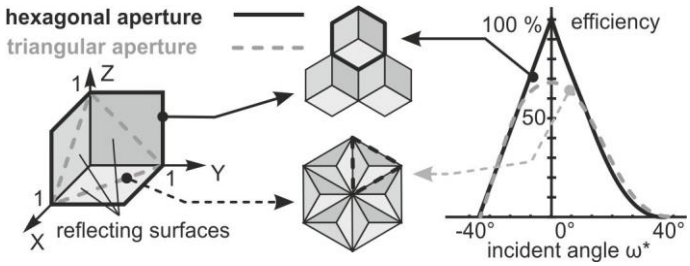

Figure 1: Reflectivity of retroreflectors with hexagonal and triangular aperture cf. [14].

Another important factor in machining highly efficient hexagonal retroreflectors is the angular accuracy between the mirror facets. A maximum deviation of 0.05° is demanded in the patent of Stamm [15] for automotive applications, while the deviations for free space communication systems are extensively discussed by Zhu et al. [16].

2 Diamond Micro Chiseling

While a downscaling of structure size is possible for arrays of triangular retroreflectors using diamond milling [14, 17] or grooving [18] processes, this is a challenging task for hexagonal retroreflector arrays, due to the absence of continuous tool paths, as the commonly used pin-building techniques are not applicable. In this case, the concave sharp edges cannot be machined by processes based on rotational motions (e.g. turning or milling) [19]. Thus, the Diamond Micro Chiseling (DMC) process has been developed, for machining arbitrary prismatic microcavities of which miniaturized hexagonal retroreflector arrays in a size between 50 and 500 µm [20] can be generated.

2.1 Tool geometry

The DMC process relies on dedicated V-shaped monocrystalline diamond tools. In comparison to conventional diamond tools used for turning or milling operations, the DMC tools are operated 90° rotated around the shaft axis while maintaining the cutting direction of conventional tools. This results in a switched alignment of rake and flank face and consequently a completely different configuration of

the cutting edges and tool angles. The characteristics of the diamond tools used for Diamond Micro Chiseling are shown in Figure 2.

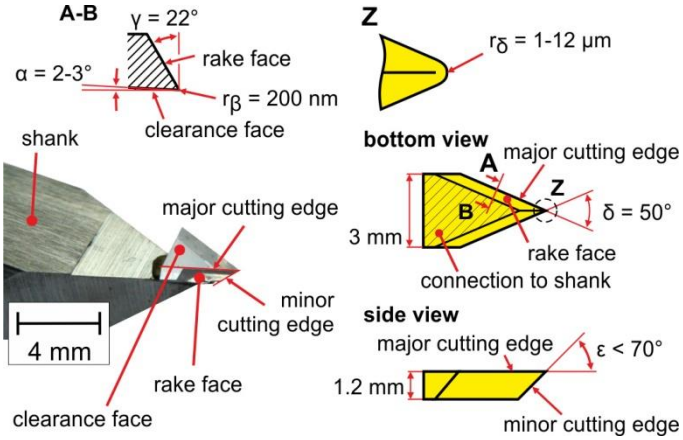

Figure 2: V-shaped diamond tool dedicated for the Diamond Micro Chiseling process.

While in theory a sharp edged tool is necessary for generating perfect prismatic microcavities, most tools designed for Diamond Micro Chiseling feature a rounded nose with a radius of r_δ = 1-12 µm for stability reasons. Some DMC tools also feature a rounded cutting edge (r_β = 200-300 nm), which further improves the stability of the tool and is mainly used for rough cutting purposes. In order to minimize the necessary effort for tool alignment, intrinsic rake (γ = 22°) and clearance (α = 2-3°) angles are ground into the diamond thus only making it necessary to align certain reference planes on the shank within the machine tool. The opening angle (δ = 50°) and the corner angle (ε = 70°) of the tool determine the machinable geometric spectrum of the microcavities. Due to the quasi-symmetric geometry of the tool, there is a certain dependency between the angles of the diamond tool. For example, decreasing the rake angle results in an enlarged corner angle and thus reduces the machinable geometric spectrum. This could be avoided by utilizing an asymmetric tool design which, however, further increases the complexity and costs of the already expensive tools.

2.2 Machine setup and process kinematics

An ultraprecision machine tool with at least five numerically controlled axes (three linear and two rotational) is required for the Diamond Micro Chiseling process (Figure 3).

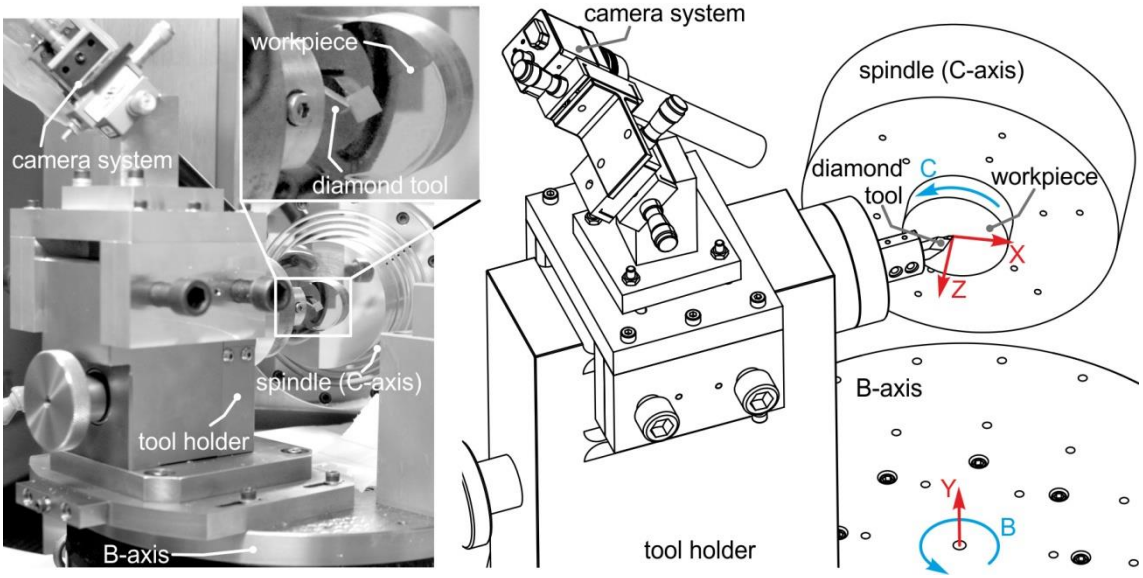

Figure 3: Machine setup for Diamond Micro Chiseling on a Nanotech 350FG (left: photography of setup, right: schematic wireframe image).

One of the rotational axes (B) is used for setting the inclination angle (χ) of the tool relative to the workpiece, while the second one (C) is used to rotate the workpiece itself. The linear axes (X, Y and Z) are used for positioning the tool relative to the workpiece and for executing the cutting motion.

In the first step, the tool plunges into the surface in [-X Y -Z] direction until the apex of the cavity is reached and is then retracted from the surface in [X Y Z] direction (see Figure 4). Hence, a single mirror facet with triangular geometry is generated which has an inclination angle equal to χ. For cutting the next facet, the workpiece has to be rotated and the tool repositioned to the endpoint of the previous cut. This procedure is continued until the starting point of the first cut is reached and the chip is separated from the cavity. To minimize the stress on the diamond tool, the structures have to be cut in several layers with constant chip thickness [21]. Therefore, a stack of identical cavities is machined with decreasing offset in Z direction.

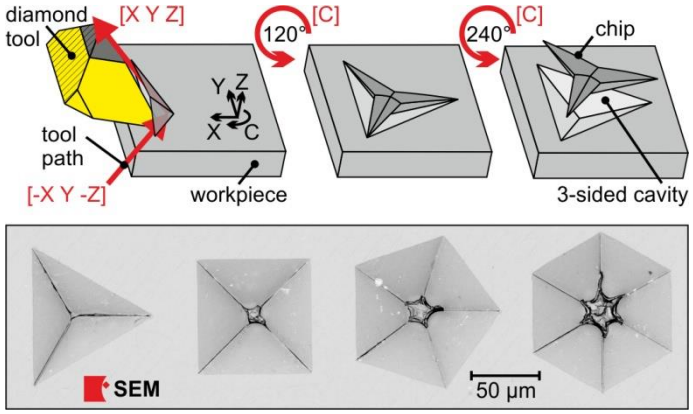

Figure 4: Kinematics for machining a 3-sided cavity and exemplary structures.

In order to form truly sharp edged cavities, the machine axes have to perform many discontinuous movements without parasitic influences due to acceleration and deceleration. As the control system of most CNC lathes is designed for speed on rather continuous motions, it tends to interpolate between the defined points thereby rounding the sharp edges. Additionally, fast acceleration and deceleration of the machining axes induces vibrations into the system which have an impact on the achievable quality of the structure. Without touching the control system itself, these unwanted effects can be avoided by choosing relatively low cutting and positioning speeds and by introducing additional in-position checks (i.e. dwell time) in the CNC program.

2.3 Tool alignment

As the chip is only separated from the cavity if the boundaries of the individual cuts meet with a high accuracy, the precise alignment of the tool is crucial to the success of the process. Therefore, the developed alignment procedure is divided into four steps which need to be repeated in an iterative cycle until the desired form accuracy is achieved.

In the first step, the tool shank is aligned parallel to the YZ-plane of the machine in order to be able to set the inclination angle (χ) of the tool using the B-axis. If the angular position of the cutting edge is known with respect to the shank, this typically results in an angular accuracy < 0.5°. An alternate method is to align the cutting edge almost parallel to the surface of the workpiece and then to cut a step profile by turning or grooving operations. According to the relative angular position of the workpiece' surface and the step profile, the deviation of the inclination angle can be determined by tactile or optical metrology. It is important that the surface of the workpiece has a defined orientation with respect to the machine axes, which can be achieved by facing the surface prior to cutting the step profile (i.e. diamond turning using a standard diamond tool). The machining of the step profile, however, puts further stress on the DMC diamond tool and is only used when high demands in angular precision (as for retroreflectors) have to be met. Initial experiments have shown that an accuracy of < 0.01° can be reached using this method (see Figure 5), however further evaluations have to be conducted to ensure the repeatability of this method.

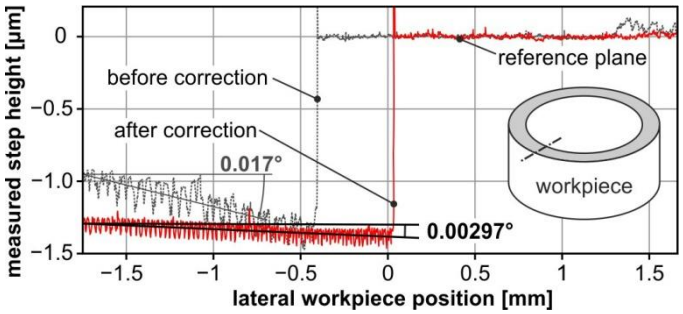

Figure 5: Measurement of the inclination angle of the cutting edge by evaluating turned step structure.

In the second step, the contact point between tooltip and workpiece has to be determined by adjusting the Z-position of the tool. This is necessary as the depth of cut influences the stress on the diamond and also the form accuracy (depth and width) of the microcavities. A coarse alignment is done by observing the tooltip and its reflection on the workpiece using the camera system shown in Figure 3. The Z-position is then corrected by moving to tool towards the surface in discrete steps until cutting marks can be observed. According to the number of cutting marks and the moved steps, it is possible to set the Z-position of the tool with accuracy in the range of the step size, which usually is 250 nm.

The third step is concerned with aligning the diamond tool to the rotational center (C-axis) of the main spindle. For this, dedicated alignment structures have been developed, consisting of two symmetric parts, which ideally form a square (see Figure 6). In Y-direction, a continuous cut can be machined, as it coincides with the intended cutting direction of the tool. In X-direction, discrete cutting marks, comparable to those of the Z-alignment, have to be machined and are interpolated linearly during measurement.

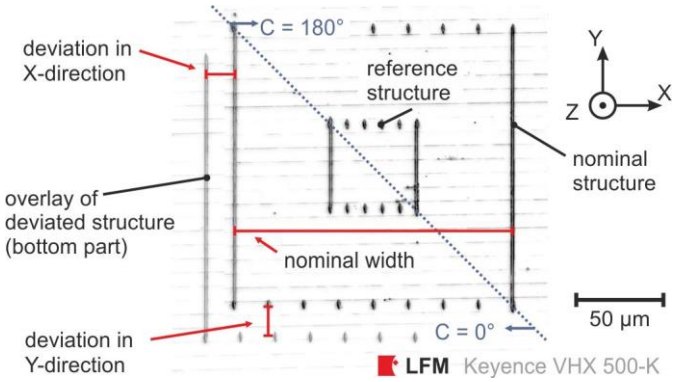

Figure 6: Alignment structure for XY-positioning of the DMC diamond tool.

One L-shaped half of the alignment structure is machined at zero rotation of the C-axis. A second L-shaped half is machined at a fixed distance to the first one as a reference for automated measurements. The other half of the squares is machined after rotating the C-axis by 180° and repositioning of the tool to the nominal position of the first half. If the tool is not precisely aligned on the rotational center, the resulting squares are misaligned. The deviation is measured using a calibrated video microscope and used for compensating the tool's position.

In the last step, cavities are machined into the workpiece using the DMC process. These are evaluated for dimensional and angular accuracy and if necessary, the inclination angle of the tool is corrected by rotating the B-axis. An example for an angular deviation can be seen in Figure 7. The left SEM picture shows an array with a misalignment of approx. 1°. As the actual inclination angle of the tool is steeper than the nominal angle, the facets do not meet at the convex peaks of the retroreflective pattern and thus form a triangular plateau. Due to deviations in positioning the tooltip on the rotational center of the B-axis (this error cannot be compensated by moving the machine's axes) the whole alignment procedure has to be repeated until the desired values for the inclination angle are achieved.

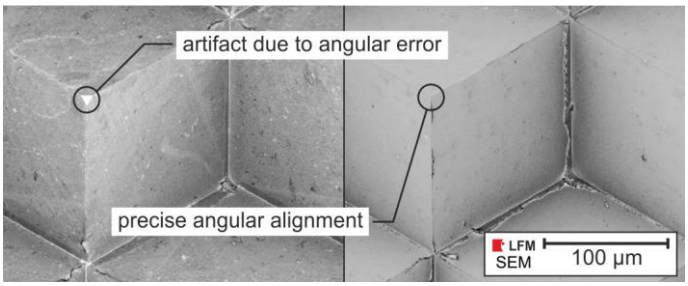

Figure 7: Triangular plateaus as an artifact resulting from angular deviation of the B-axis.

3 Cutting strategies for large-scale retroreflective arrays

Triple mirrors require a three-sided cavity with an inclination angle of $\chi = 54.74°$. When machining multiple of these cavities in an overlapping fashion, a hexagonal cube corner is obtained (Figure 8).

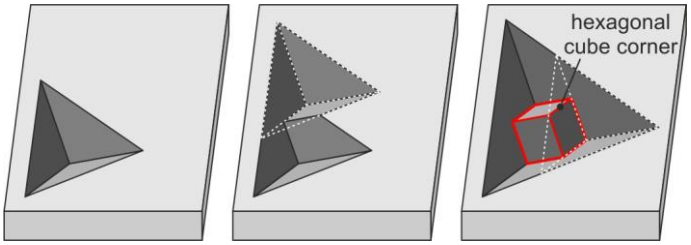

Figure 8: Cutting a mold for a cube corner retroreflector by overlapping three triangular cavities.

3.1 Analysis of exemplary retroreflective patterns

In order to analyze the major influences on total machining time, the required process time has been divided into four different categories: The first is the actual time in which material is removed ('cutting time'). The second is the time which is required to reposition the diamond tool to the start points of the facets after rotating the workpiece to the subsequent orientation (compare chapter 2.2) and thus is called 'positioning time'. The third category is the time needed for the rotation of the workpiece by the machine's spindle ('rotation time'). All other operations not falling into one these categories (position checks, spray mist bursts etc.) are categorized as 'overhead time'.

As an example, the process for Diamond Micro Chiseling a 5 x 5 mm² array with a characteristic structure dimension of 150 µm (i.e. 1216 structures) is analyzed using a software tool which implements the DMC kinematics and estimates the total process time on the basis of the length of the toolpath and the applied feedrate. For this analysis, an undeformed chip thickness of h = 4 µm is chosen, resulting in a pattern of 69312 discrete cuts with a total length of 16.5 m. At a maximum cutting speed of v_c = 60 mm/min the total process time sums up to around 146 h with nearly 45 % of this time being used for rotating the workpiece and another 24 % for repositioning the tool. During this time, the cutting conditions have to be monitored and the machine tool and its environment have to be kept as stable as possible.

Industrial applications, however, require the structuring of seamless areas (i.e. not composed of smaller patterns) which are significantly larger than at least 10 x 10 mm² for direct use in measurement applications. In terms of the amount of structures and thus the required machining time, these 100 mm² are already a 'large' area. Hence, dedicated cutting strategies have to be applied to enable a feasible structuring of large surfaces:

1. Reduction of workpiece rotations and thus tool repositioning time by concatenating cuts with the same orientation.
2. Minimization of the toolpath by changing the simple "stacking" of cavities to cutting individually sized cavities for each layer (i.e. avoiding air cuts).

3. Truncation of adjacent cuts by connecting their intersection points and omitting nonessential motions.
4. Performance of in-situ tool changes to perform rough cutting with large undeformed chip thickness/high cutting speed and finish cutting with finer tools and quality related machining parameters.
5. Reduction of non-productive process time by utilizing semi-automated tool alignment procedures.
6. Improvement of machine stability and control behavior for minimizing vibrations induced by changes of speed and direction at the corners of the discontinuous tool path.

The principle ideas of strategies one to three are illustrated in Figure 9.

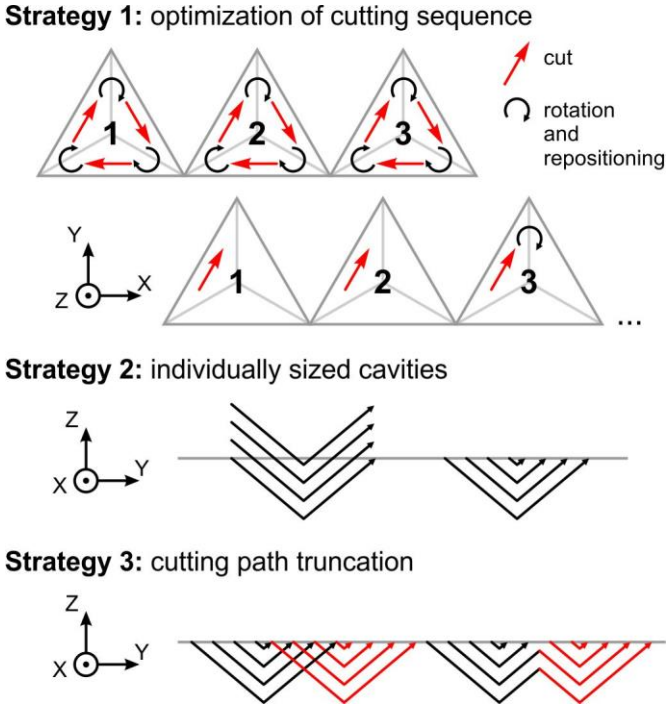

Figure 9: Optimization strategies for Diamond Micro Chiseling.

3.2 Optimizations of cutting sequence and structure geometry

Implementing the first of these strategies, by adding all individual cuts to a list and then sorting this list according to the required angular position, results in a decrease of process time to 65 h with only 0.1 % being required for rotation of the C-axis. The rest of the time is equally distributed to the other categories. The second strategy impacts on the cutting time by reducing the total path length and reduces the estimated process time to 57 h.

Strategy number three aims to eliminate positioning and overhead time by connecting intersecting cuts. As a consequence, the tool does not have to be retracted from the workpiece between cuts and thus the need for additional stops and position checks is obsolete. Yet, a high contouring accuracy is attained as the cutting speed is kept at a low rate. Applying this strategy leads to a total process time of 33 h. This time can be further reduced to a minimum value of 18 h by applying strategy 3 not only to intersecting cuts, but to all adjacent facets in cutting direction.

The effects of strategies one to three are depicted in Figure 10. Utilizing these strategies, the structuring areas of up to 15 x 15 mm² become feasible. Larger patterns, however, still require extensive machining time as the amount of structures is increasing quadratic with the increase in structured area.

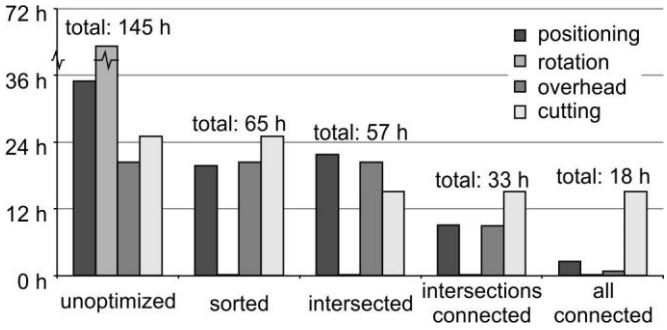

Figure 10: Effects of optimization strategies on cutting time for a 5 x 5 mm² hexagonal retroreflector array with a structure size of 150 µm.

3.3 In-situ tool changes

By performing an in-situ tool change, as described in strategy four, different tools can be utilized for rough and finish cutting. Thus, rough cutting tools are optimized for high material removal rates by applying a comparably large nose radius as well as a rounded cutting edge, in order to prevent chipping while applying a high undeformed chip thickness. Finishing tools, on the other hand, are optimized for contouring accuracy and optimum surface roughness and are only used for machining the final surface of the cavity.

An in-situ tool change, however, always implies a new tool alignment which is time consuming and introduces additional uncertainties into the process: The novel tool has to be precisely aligned to the angular and lateral position of the previous tool; otherwise the structuring process cannot be continued within the already machined cavities. This has to be done within the range of the undeformed chip thickness applied for the finishing layers which is in the range of 1-3 µm. By using the procedure described in 2.3 the tooltip is always aligned to the rotational center of the C-axis. Thus, the required accuracy is automatically achieved as long as the workpiece is not dismounted from the C-axis.

Several attempts have been made to improve the accuracy and speed of the tool alignment procedure. Using a telecentric lens system and a CCD camera, it was possible to calculate the tool correction factors using image recognition techniques on the alignment structures shown in Figure 6. In initial experiments, setting the deviation of the alignment structures to known values, the correction factors could be calculated with a repeatability of <1 µm in a few milliseconds.

4 Experimental results

4.1 Identification of mold material

For evaluating the performance of the DMC process, groove type structures have been machined in different workpiece materials while varying the undeformed chip thickness and the cutting speed of the process. Electroless nickel (NiP), nickel silver N31 (CuNi7Zn39Pb3Mn2) and oxygen free high conductivity (OFHC) copper were utilized by Flucke et al. to characterize the fundamental process behavior [21]. In different experiments, the undeformed chip thickness was varied while keeping the cutting speed constant and vice versa. For determining the process performance, the surface roughness and waviness of the mirror facets were measured using a profilometer. It was shown that the best surface quality and form accuracy is achieved at minimal undeformed chip thickness ($h < 3$ µm, see Figure 11 and Figure 12, left diagrams) and extremely low cutting speeds ($v_c < 100$ µm/s, see Figure 13 and Figure 14, left diagrams) and in the finishing layer.

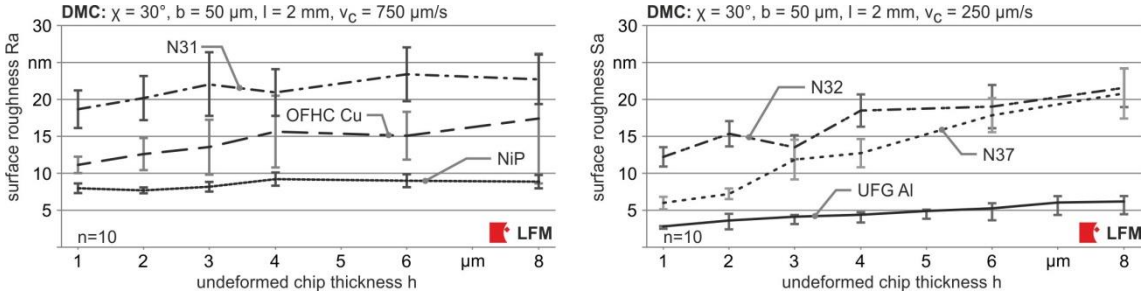

Figure 11: Surface roughness against undeformed chip thickness. Left: electroless nickel, copper and nickel silver N31 (courtesy of Flucke et al.); Right: novel results on nickel silver N32/N37 and UFG aluminum.

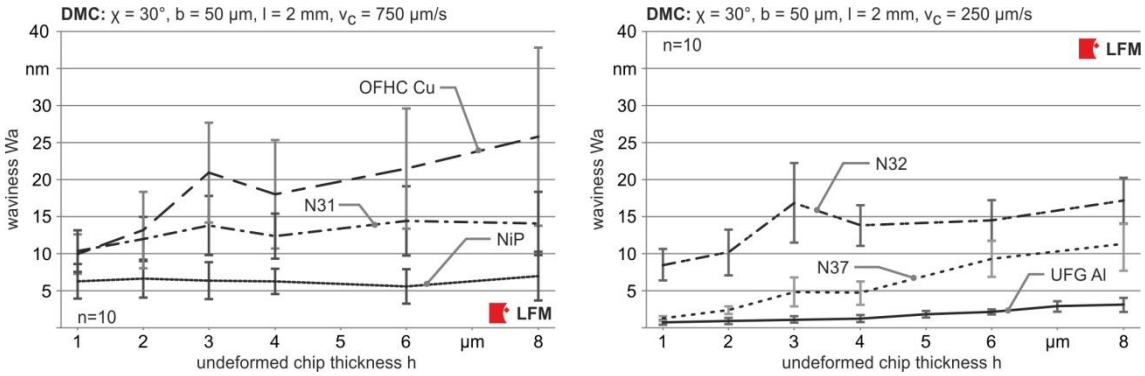

Figure 12: Waviness against undeformed chip thickness. Left: electroless nickel, copper and nickel silver N31 (courtesy of Flucke et al.); Right: novel results on nickel silver N32/N37 and UFG aluminum.

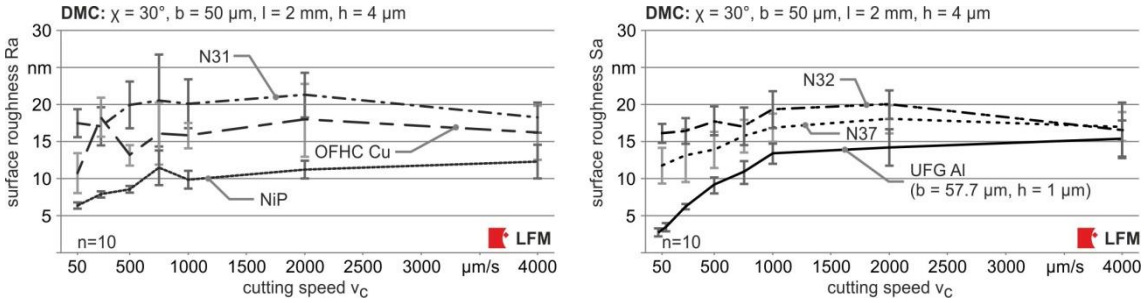

Figure 13: Surface roughness against cutting speed. Left: electroless nickel, copper and nickel silver N31 (courtesy of Flucke et al.); Right: novel results on nickel silver N32/N37 and UFG aluminum.

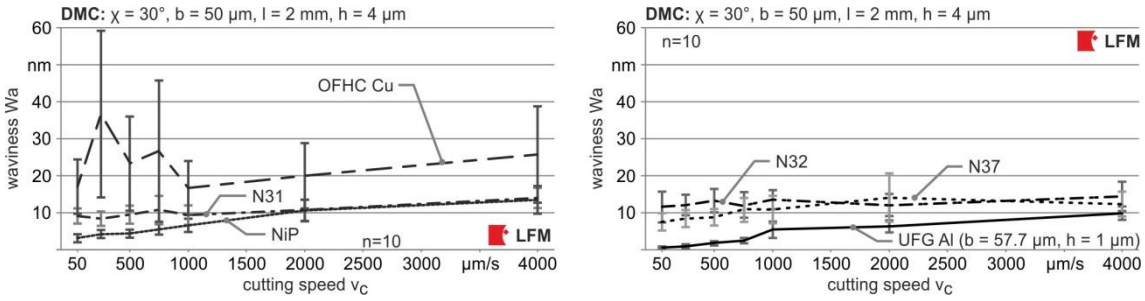

Figure 14: Waviness against cutting speed. Left: electroless nickel, copper and nickel silver N31 (courtesy of Flucke et al.); Right: novel results on nickel silver N32/N37 and UFG aluminum.

The best achievable surface roughness of the OFHC copper sample was measured to Ra = 10.78 nm ±2.71 nm, while the nickel silver N31 sample also yielded non-optical surface finish (Ra = 17.10 nm ±2.56 nm). The best results of these three materials were achieved for electroless nickel plating, which yielded an optical surface finish of Ra = 6.41 nm ±0.42 nm. Nevertheless, it is unsuitable for machining large-scale retroreflective arrays as it results in catastrophic tool wear even after short cutting distances.

Thus novel materials have been investigated for their applicability as a microstructurable mold material. The spectrum of investigated materials consists of two nickel silver alloys N32 (CuNi12Zn30Pb1) and N37 (CuNi18Zn19Pb1) suitable for precision machining (cf. [22]) and aluminum Al1070 (Al > 99.7%) with ultra

fine grain structure (UFG-Al). The latter is produced by equal channel angular pressing, a method of severe plastic deformation used for generating nanostructured metals which is described by Olejnik et al. [23].

All materials were structured with a parameter-variation similar to that of the previous investigation. Only minor improvements of the base parameters (i.e. slightly reduced cutting speed) were made as a consequence of the findings of the preceding tests. To obtain a more holistic view of the mirror facets, the roughness and waviness measurements were conducted using white light interferometry. The size of the evaluated area (50 x 300 µm²) and the filtering operations (gaussian with 80 µm cutoff used as highpass for obtaining the arithmetic mean height and as lowpass for obtaining the waviness) were chosen in a way that both measurements are comparable.

While nickel silver N32 yields insufficient surface quality (Sa = 12.31 nm ±1.27 nm at best) within the applicable set of parameters, it was found that the N37 alloy can be microstructured with a surface finish comparable to that of electroless nickel (Sa = 5.91 nm ±0.85 nm), but at significantly lower tool wear. Even by using a large undeformed chip thickness of h = 8 µm resulted in negligible tool wear after cutting structures with a total length of 40 m, which is equivalent to cutting a 10 x 10 mm² retroreflector array with a structure size of 150 µm.

The best results in terms of surface roughness and waviness were achieved by Diamond Micro Chiseling of UFG aluminum. With a surface roughness down to Sa = 2.87 nm ±0.17 nm and a waviness of Wa = 0.84 ±0.38 nm it outperforms the results of electroless nickel for the variation of the undeformed chip thickness (see Figure 11 and Figure 12). On the other hand, UFG aluminum is much more susceptible to increased cutting speed, as can be seen in Figure 13 (right). Despite the remarkable results for direct machining, its applicability as a mold material has not been tested yet.

4.2 Machining of large-scale retroreflective arrays

Using optimization strategies one, four and six described above, it was possible to machine a highly efficient retroreflective array with a structure size of 200 µm covering an area of 10 x 10 mm² on a nickel silver N37 mold. At first, a rough cut, using a r_δ = 12 µm tool with rounded cutting edge was carried out. After cutting 18 layers with h = 5 µm and v_c = 45 mm/min, a tool change to a r_δ = 1 µm, sharp edged diamond tool was performed. The finish cut was done in three layers (h = 2 µm; 1.28 µm and 1 µm) with v_c = 15 mm/min.

The total process time was approx. 200 hours, including the times for alignment of the abovementioned diamond tools. The SEM image depicted on the left side in Figure 15 show, that a homogenous optical quality was achieved across the entire surface.

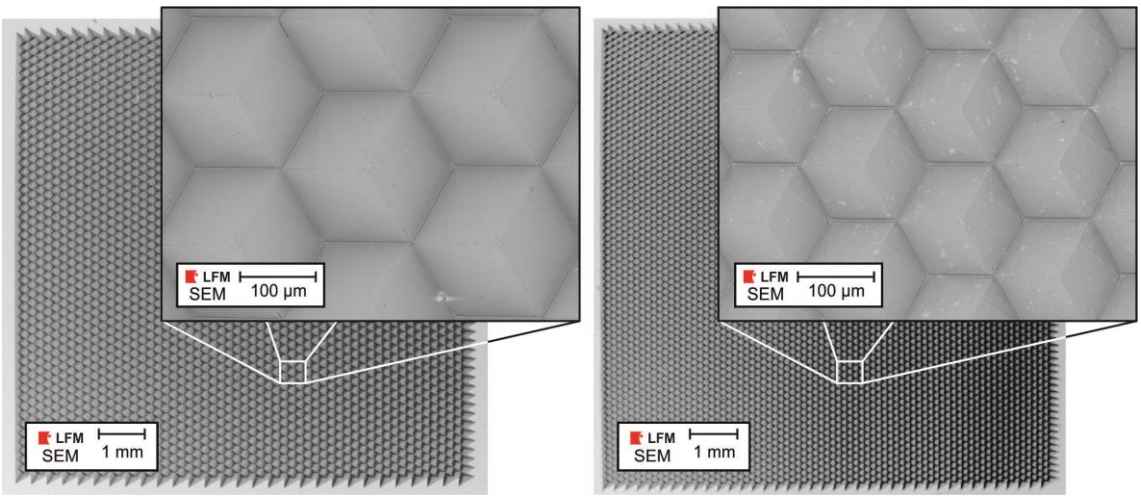

Figure 15: 10 x 10 mm² cube corner arrays with a structure size of 200 µm (left) and 150 µm (right).

Evaluating the angular deviation of the retroreflective array, however, is a challenging task, as the measurement techniques utilized for large retroreflectors (e.g. direct interferometric measurement) cannot be applied on this scale. Thus, the optical performance of the retroreflective surface was

evaluated using a reflection measurement system. This system illuminates the sample from different angular positions and measures the luminance intensity according to various standards. According to the peak value of the intensity curve, the deviation of the incident to the reflected ray can be determined and recalculated to the angular deviation of the retroreflectors. Both mold and replicated optics were evaluated in this way. The peak value for the plastic optics exhibited slightly higher values than those of the metal optics due to refraction and form error within the replica. According to these measurements, the relative angular deviation of the cube corner facets was calculated to 0.1°. This is mainly because the advanced tool setting techniques for B-axis alignment have not yet been applied in this experiment. Despite the fact that the angular deviation is out of the desired range for the application, the overall luminance intensity was up to 50% higher than comparable structures with triangular geometry.

In a later experiment, a retroreflector mold with a structure size of 150 µm and a pattern size of 10 x 10 mm² (i.e. more than 5000 cube corners) was machined (see Figure 15, right). This time, the optimization strategies two and three had been implemented into the CAM system resulting in a total process time of 95 h. Additionally, the advanced tool setting procedure was used to set the tool inclination angle with an accuracy of 0.02° within the machine tool. The cutting was conducted using a single tool with r_δ = 1.23 µm and a sharp cutting edge dividing the structures into 17 layers with h = 4 µm, one layer with h = 1.71 µm and a final layer with h = 1 µm. The applied cutting speed was v_c = 45 mm/min for layers 1 to 17 and v_c = 3 mm/min for the last two layers.

In spite of the novel tool setting method and therefore higher angular accuracy, the optical performance of the second reflector was not significantly increased. To examine this issue, diffraction patterns were recorded for both samples using a coherent light source. These patterns exhibited maxima of higher orders, a behavior unknown for hexagonal retroreflectors. A possible explanation is, that a diffraction grating is formed, represented by the homogenous distribution of the cube corners with minor angular deviations in combination with the small structure size. However, further research has to be conducted in order to verify this thesis.

5 Short summary and outlook

In this paper, the latest results of the Diamond Micro Chiseling process have been presented, focusing on the machining of large scale structures such as micro-retroreflectors. The geometry of the applied diamond tools have been presented along with the machine setup and the required cutting kinematics. Particular attention was given to the measurement procedures for the alignment of the diamond tool within the ultraprecision machine tool. Furthermore, specific strategies for minimizing the required machining time were presented.

From various cutting experiments and surface characterization, electroless nickel, nickel silver N37 and UFG aluminum were identified as suitable materials for machining optical microstructures on a small scale. However, when machining larger patterns on mold inserts, the choice of materials is limited to N37 as the machining exhibits negligible tool wear.

Thus, nickel silver N37 was used for Diamond Micro Chiseling of two 10 x 10 mm² retroreflective arrays which were replicated into plastic optics and then measured for optical functionality. The first array had a structure size of 200 µm and a relative angular deviation of the mirror facets of 0.1°. The second array not only featured a smaller structure size (150 µm), but was machined by implementing the machining and tool setting strategies described in this paper. This resulted in a reduction of machining time to approximately 50 % and a reduced angular deviation to approximately 0.02°. However, this array showed unexpected diffraction behavior as it possibly acts as a diffraction grating.

In the ongoing research, further experiments will be conducted to evaluate functional performance of retroreflective arrays generated by Diamond Micro Chiseling. Particular attention will be given to the diffraction behavior of the machined structures.

Accepted manuscript, DOI of final publication: 10.1016/j.precisioneng.2012.06.001

6 Acknowledgement

The authors like to thank the German Research Foundation (DFG) for funding this work as a part of the Transregional Collaborative Research Center SFB/TR4 “Process Chains for the Replication of Complex Optical Elements”.

The authors also thank the company IMOS Gubela GmbH for their work in replicating the retroreflective arrays and testing their optical functionality as part of a joint research project.

7 References

[1] Denkena B, Ostermann J, Becker C, Spille C. Mechanical information storage by use of an excited turning tool. Prod Eng. 2007;1:25-30.
[2] Klocke F, Feldhaus B, Mader S. Development of an incremental rolling process for the production of defined riblet surface structures. Prod Eng. 2007;1:233-237.
[3] Biermann D, Surmann T, Odendahl S, Steiner M, Hense R, Rausch S. Creating Functional Surface Structures by Milling using Self-Excited Tool Vibrations. ASPE Spring Topical Meeting "Structured and Freeform Surfaces". 2011;51:55-58.
[4] Evans CJ, Bryan JB. "Structured", "Textured" or "Engineered" Surfaces. CIRP Annals. 1999;48:541-556.
[5] De Chiffre L, Kunzmann H, Peggs GN, Lucca DA. Surfaces in Precision Engineering, Microengineering and Nanotechnology. CIRP Annals. 2003;52:561-577.
[6] Bruzzone AAG, Costa HL, Lonardo PM, Lucca DA. Advances in engineered surfaces for functional performance. CIRP Annals. 2008;57:750-769.
[7] Luoma J, Schumann J, Traube EC. Effects of retroreflector positioning on nighttime recognition of pedestrians. Accident Analysis & Prevention. 1996;28:377-383.
[8] Rabinovich WS, Mahon R, Goetz PG, Waluschka E, Katzer DS, Binari SC, et al. A cat's eye multiple quantum-well modulating retro-reflector. Photonics Technology Letters, IEEE. 2003;15:461-463.
[9] Estler WT, Edmundson KL, Peggs GN, Parker DH. Large-Scale Metrology - An Update. CIRP Annals. 2002;51:587-609.
[10] Liepmann TW. How retroreflectors bring the light back. Laser Focus World. 1994;30:129.
[11] Seward GH, Cort PS. Measurement and characterization of angular reflectance for cube-corners and microspheres. Optical Engineering. 1999;38:164-169.
[12] Kim H, Lee B. Optimal design of retroreflection corner-cube sheets by geometric optics analysis. Optical Engineering. 2007;46:094002-094001-094014.
[13] Eckard HD. Simple Model of Corner Reflector Phenomena. Appl Opt. 1971;10:1559-1566.
[14] Autschbach L, Brinksmeier E, Gubela H-E, Ahbe T. Manufacturing of three-dimensional micro-optic functional surfaces. HTM. 2005;1:33-39.
[15] Stamm RF, inventor American Cyanamid Company, assignee. Retroreflective Surface. USA patent 3,712,706. 1973.
[16] Zhu X, Hsu VS, Kahn JM. Optical modeling of MEMS corner cube retroreflectors with misalignment and nonflatness. Selected Topics in Quantum Electronics, IEEE Journal of. 2002;8:26-32.
[17] Luttrell DE. Novel use of a traditional machining method for generation of large scale micro-structured surfaces. ASPE Spring Topical Meeting "Structured and Freeform Surfaces". 2011;51:143-146.
[18] Moriya T, Nakamoto K, Ishida T, Takeuchi Y. Creation of V-shaped microgrooves with flat-ends by 6-axis control ultraprecision machining. CIRP Annals. 2010;59:61-66.
[19] Denkena B, Boehnke D, Kästner J. Microstructuring of functional surfaces by means of cutting processes. Prod Eng. 2008;2:21-25.
[20] Brinksmeier E, Gläbe R, Flucke C. Manufacturing of molds for replication of micro cube corner retroreflectors. Prod Eng. 2008;2:33-38.
[21] Flucke C, Gläbe R, Brinksmeier E. Diamond Micro Chiselling of Molding Inserts for Optical Micro Structures. 23th ASPE Annual Meeting and 12th ICPE. 2008;44:92-95.
[22] Brinksmeier E, Schönemann L, Gläbe R. Review on Diamond-Machining Processes for the Generation of Functional Surface Structures. 4th CIRP HPC conference. 2010;1:79-84.
[23] Olejnik L, Rosochowski A. Methods of fabricating metals for nano-technology. Bulletin of the Polish Academy of Sciences. 2005;53:413-423.